Mark D. Shenderovich
Katalin E. Kövér*
Department of Chemistry
University of Arizona
Tucson, AZ 85721

Gregory V. Nikiforovich
Center for Molecular Design
Washington University
St. Louis, MO 63130

Ding Jiao†
Victor J. Hruby‡
Department of Chemistry
University of Arizona
Tucson, AZ 85721

Conformational Analysis of β-Methyl-*para*-Nitrophenylalanine Stereoisomers of *cyclo*[D-Pen^2, D-Pen^5]enkephalin by NMR Spectroscopy and Conformational Energy Calculations

*Solution conformations of β-methyl-*para*-nitrophenylalanine^4 analogues of the potent δ-opioid peptide* cyclo[D-*Pen*^{2}, D-*Pen*^{5}]*enkephalin (DPDPE) were studied by combined use of nmr and conformational energy calculations. Nuclear Overhauser effect connectivities and* $^3J_{HNC^{\alpha}H}$ *coupling constants measured for the (2S, 3S)-, (2S, 3R)-, and (2R, 3R)-stereoisomers of* [β-*Me*-p-NO_2*Phe*^{4}]*DPDPE in DMSO were compared with low energy conformers obtained by energy minimization in the Empirical Conformational Energy Program for Peptides (ECEPP/2) force field. The conformers that satisfied all available nmr data were selected as probable solution conformations of these peptides. Side-chain rotamer populations, established using homonuclear (*$^3J_{H^{\alpha}H^{\beta}}$*) and heteronuclear (*$^3J_{H^{\alpha}C^{\gamma}}$*) coupling constants and* ^{13}C *chemical shifts, show that the β-methyl substituent eliminates one of the three staggered rotamers of the torsion angle* χ^1 *for each stereoisomer of the β-Me-*p-NO_2*Phe*^{4}*. Similar solution conformations were suggested for the* L-*Phe*^{4}*-containing (2S, 3S)- and (2S, 3R)-stereoisomers. Despite some local differences, solution conformations of* L- *and* D-*Phe*^{4}*-containing analogues have a common shape of the peptide backbone and allow similar orientations of the main δ-opioid pharmacophores. This type of structure differs from several models of the solution conformations of DPDPE, and from the model of biologically active conformations of DPDPE suggested earlier. The latter model is allowed for the potent (2S, 3S)- and (2S, 3R)-stereoisomers of* [β-*Me*-p-NO_2*Phe*^{4}]*DPDPE, but it is forbidden for the less active (2R, 3R)- and (2R, 3S)-stereoisomers. It was concluded that the biologically active stereoisomers of* [β-*Me*-p-NO_2*Phe*^{4}]*DPDPE in the δ-receptor-bound state may assume a conformation different from their favorable conformations in DMSO.* © *1996 John Wiley & Sons, Inc.*

Received December 7, 1994; accepted May 19, 1995.

* Present address: Biogal Pharmaceutical Works, H-4042 Debrecen, Hungary.

† Present address: Section of Nucleic Acid Chemistry, Division of Chemical Carcinogenesis, American Health Foundation, Valhalla, NY 10595.

‡ To whom correspondence should be addressed.

Biopolymers, Vol. 38, 141–156 (1996)

CCC 0006-3525/96/020141-16

INTRODUCTION

cyclo[D-Pen^2, D-Pen^5]enkephalin (DPDPE), a conformationally constrained synthetic analogue of enkephalin with the amino acid sequence H-Tyr^1-D-Pen^2-Gly^3-Phe^4-D-Pen^5-OH, has been found to be one of the most selective and potent δ-opioid peptides.[1] Several studies have been aimed at obtaining possible solution and receptor-bound conformations of DPDPE using both nmr spectroscopy[2,3] and a variety of theoretical methods.[4–13] It was shown that a limited number of conformers are sterically allowed for the 14-membered disulfide ring of DPDPE,[9,11] while the acyclic tyrosine residue and the phenylalanine side-chain moieties retain considerable conformational mobility. Recent x-ray studies[14] revealed a conformational diversity in the acyclic part of DPDPE even in the crystal state, since three molecules with different orientations of the Tyr^1 residue were found within the same crystal unit. Due to the mobility of these critical functional groups, the establishment of an exact three-dimensional arrangement for the δ-receptor pharmacophore of DPDPE remains a challenging problem. Several conformation–activity studies,[6–10,13,15] in which different series of δ-opioid peptides were compared, resulted in different models for the biologically active conformation of DPDPE. Therefore, a second generation of analogues,[16,17] which were aimed at constraining the tyrosine or phenylalanine side chains of DPDPE, are of a special interest for experimental and theoretical conformational studies.

β-Methylated amino acids provide a way to obtain a better understanding of the side-chain topography of peptides required by the receptor in the recognition processes. A bulky β-methyl substituent is able to constrain conformational mobility of the modified side chain and/or bias the populations of its χ^1 torsion angle rotamers.[19] DPDPE analogues with β-methyltyrosine (β-MeTyr) and β-methylphenylalanine (β-MePhe) residues incorporated into positions 1 and 4, respectively, have shown a wide variety of opioid receptor affinities and selectivities,[16,17] depending both on the chiralities of stereoisomers and on the nature of ring substituents in the β-methylated aromatic residues. In particular, the (2S, 3S)-stereoisomer of [β-Me-*p*-NO_2Phe^4]DPDPE was as potent as the parent peptide in a δ-opioid receptor bioassay, and considerably more selective.[16]

The goals of this study were to assess the nature of the constraints imposed by the β-MePhe^4 residues on the backbone and side-chain conformations of DPDPE analogues and to correlate the solution structures of different stereoisomeric analogues with their biological activities. As a part of these efforts, a combined nmr and molecular mechanics study was carried out to determine solution structures of the (2S, 3S)-, (2S, 3R)-, and (2R, 3R)-stereoisomers of [β-Me-*p*-NO_2Phe^4]DPDPE (analogues I–III, respectively; Figure 1). Extensive sets of nmr data were obtained for these peptides in DMSO-d_6, including ^{1}H and ^{13}C chemical shifts, homo- and heteronuclear coupling constants, temperature dependence of amide proton chemical shifts, and nuclear Overhauser effect (NOE) connectivities. Comparison of the nmr data with calculated characteristics of low-energy conformers of analogues I–III allowed us to select their most probable backbone conformations in DMSO. Rotamer populations for β-Me-*p*-NO_2Phe^4 side chains were calculated using homo- and heteronuclear coupling constants, and ^{13}C chemical shifts measured for the β-methyl carbons. The solution conformations proposed here for [β-Me-*p*-NO_2-Phe^4]DPDPE analogues are compared to models of the solution,[2,3,18] crystal,[14] and biologically active[9] conformations of DPDPE suggested in previous studies. Possible relationships between solution structures and δ-receptor activities of these peptides are also discussed.

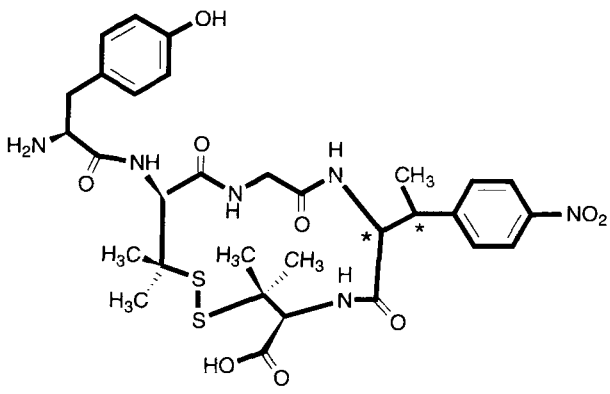

Tyr^1- D-Pen^2- Gly^3- Xxx^4- D-Pen^5- OH

Xxx: (2S,3S)-β-Me-*p*-NO_2 Phe (I)

(2S,3R)-β-Me-*p*-NO_2 Phe (II)

(2R,3R)-β-Me-*p*-NO_2 Phe (III)

(2R,3S)-β-Me-*p*-NO_2 Phe (IV)

FIGURE 1 Structure of [β-Me-*p*-NO_2Phe^4]DPDPE.

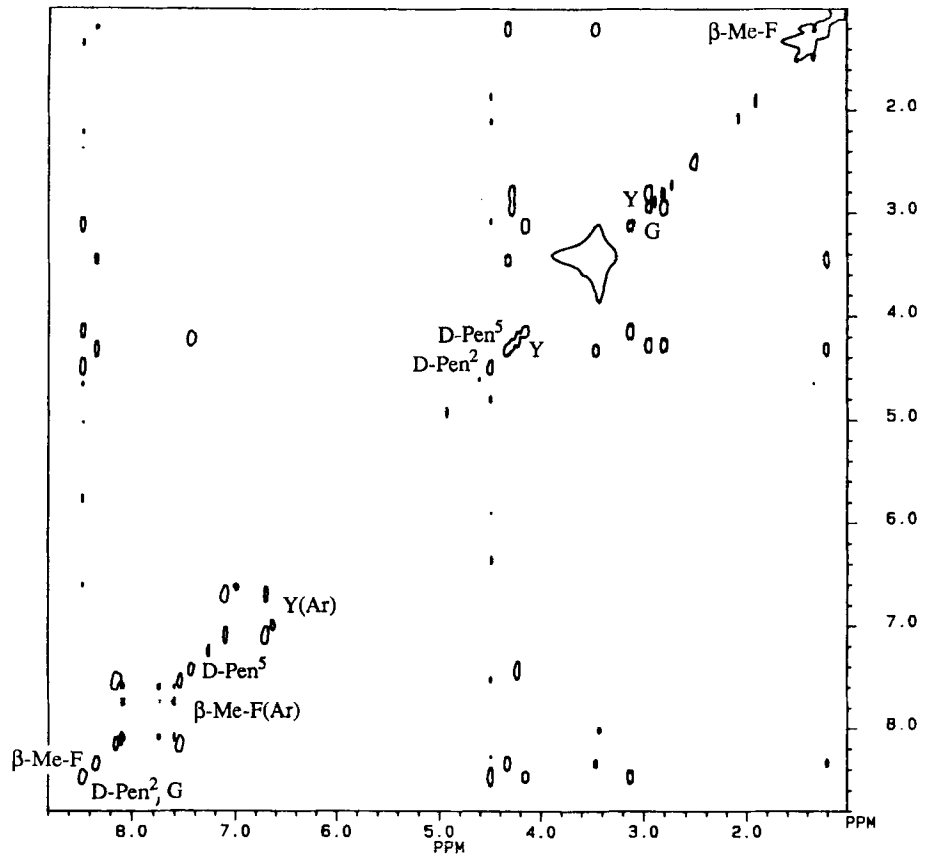

FIGURE 2 Phase-sensitive *z*-filtered ^{1}H-TOCSY spectrum of [(2S, 3S)-β-Me-*p*-NO_2Phe^4]-DPDPE in DMSO-d_6. The experimental conditions are given in Methods.

METHODS

NMR Measurements

All nmr parameters used in the present study have been obtained from one-dimensional (1D) and two-dimensional (2D) experiments[20] performed at 310 K with a BRUKER AM 500 spectrometer equipped with an ASPECT 3000 computer and a 5 mm inverse probehead. All homo- and heteronuclear experiments were carried out on peptide samples dissolved in DMSO-d_6 at a concentration of 8 mg/0.4 mL for peptides I and III, and 4 mg/0.4 mL for peptide II. The proton and carbon chemical shifts were referenced to the solvent (2.49 ppm for the residual ^{1}H signal of DMSO-d_6 and 39.5 ppm for the ^{13}C signal). Sequential assignment of proton resonances has been achieved by the combined use of *z*-filtered total correlated spectroscopy (TOCSY)[21,22] and rotating frame nuclear Overhauser effect spectroscopy (ROESY)[23,24] experiments. As an example of the assignment protocol, *z*-filtered TOCSY and ROESY spectra of peptide I are shown in Figure 2 and Figure 3, respectively. The ^{1}H chemical shifts and the conformationally important homonuclear vicinal coupling constants were extracted from the resolution enhanced 1D spectra or, in case of signal overlap, from the highly digitized 1D traces of 2D *z*-filtered TOCSY spectra. Proton detected heteronuclear spectroscopy, including *z*-filtered carbon coupled heteronuclear single-quantum correlation (HSQC)-TOCSY[25] and long-range HSQC[26] experiments, was used for the assignment of carbon resonances and for evaluation of long-range heteronuclear coupling constants $^3J_{H^\alpha C^\gamma}$ for peptides I and III. The low sample concentration of peptide II allowed only an assignment of the protonated carbons by means of a one-bond heteronuclear multiple quantum correlation[27,28] (HMQC) experiment. The experimental parameters of nmr experiments are summarized below.

Z-Filtered TOCSY. Relaxation delay 1.2 s, duration of isotropic mixing period (MLEV-17)[29] 50 ms, *z*-filter delay 15 ms, ^{1}H 90° pulse 25.5 μs, 256 experiments of 96 scans for peptides I and III, and 128 scans for peptide II, size 4 K, spectral width in F_2 and F_1 5376 Hz, quadrature detection in F_1 using TPPI,[30] zero filling in both F_1 and F_2 dimensions and multiplication with a squared cosine function. For evaluation of coupling constants, a final digital resolution of 0.3 Hz/point was achieved by inverse Fourier transformation, zero filling and back transformation of selected traces.

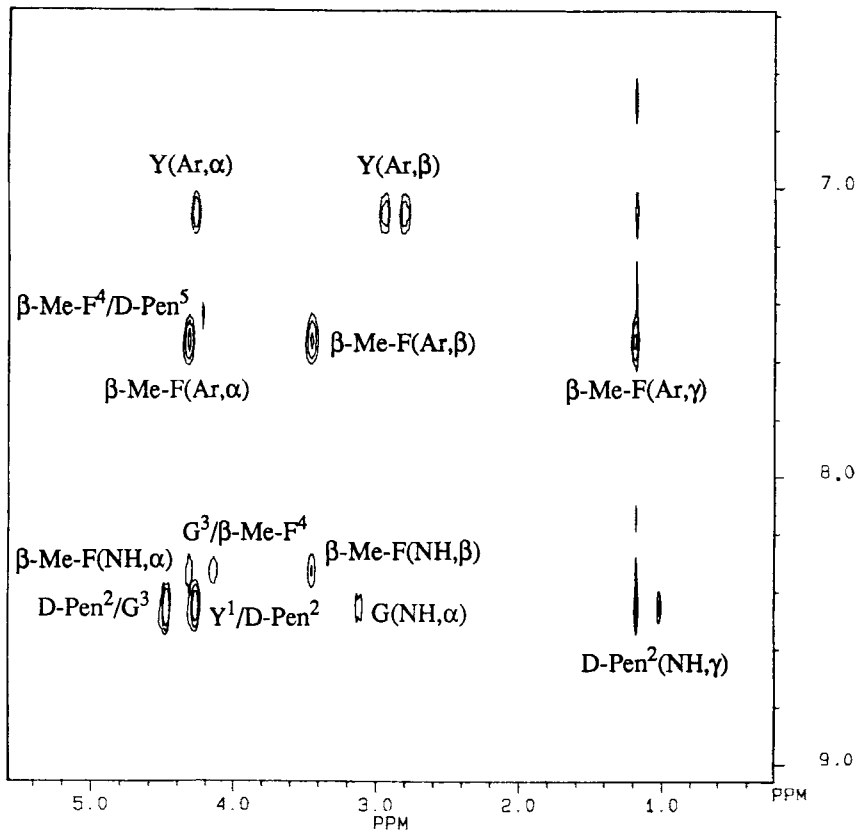

FIGURE 3 Expanded fingerprint region of the ROESY spectrum of [(2S, 3S)-β-Me-*p*-NO_2Phe^4]DPDPE in DMSO-d_6 showing the sequential connectivities.

ROESY. Relaxation delay 1.2 s, ^{1}H 90° pulse 75 μs (spin-lock field strength of 3333 Hz), duration of continuous wave (CW) spin-lock pulse 200 ms, 256 experiments of 192 scans, size 2 K, zero filling, and multiplication with squared cosine function in both dimensions.

HMQC. Relaxation delay 0.7 s, 200 experiments of 320 transients, size 2 K, spectral width 5376 Hz in ^{1}H, 16000 Hz in ^{13}C dimension, ^{1}H 90° pulse 16.5 μs, ^{13}C 90° pulse 15.2 μs, Tango spin-lock 4 ms pulses for suppression of ^{1}H-^{12}C magnetization.

Selective Long-Range HSQC. Relaxation delay 0.7 s, 110 experiments of 640 transients, size 4 K, defocusing delay 90 ms optimized for long-range couplings, spectral width in ^{13}C 5800 Hz covering the aliphatic carbon region, ^{13}C 90° pulse 33 μs with 10 dB attenuator.

Z-Filtered ^{13}C-Coupled HSQC-TOCSY. Relaxation delay 0.7 s, 240 experiments of 480 transients, size 4 K, spectral width 5376 Hz in ^{1}H, 16000 Hz in ^{13}C dimension, ^{1}H 90° pulse 16.5 μs, ^{13}C 90° pulse 15.2 μs, ^{1}H 90° pulse 25.5 μs for MLEV-17, *z*-filter delay 15 ms. The heteronuclear long-range coupling constants were obtained by comparison of the corresponding multiplet widths in the *z*-filtered homonuclear TOCSY and heteronuclear HSQC-TOCSY spectra.[25]

Side-Chain Rotamer Populations

Populations of χ^1 rotamers of Tyr^1 were estimated by Pachler's analysis of homonuclear $^3J_{H^\alpha H^\beta}$ coupling constants,[31,32] using the stereospecific assignment of β protons deduced from chemical shifts and NOE patterns. Rotamer populations of β-Me-*p*-NO_2Phe^4 side chain of peptides I and III were calculated from the homonuclear ($^3J_{H^\alpha H^\beta}$) and heteronuclear ($^3J_{H^\alpha C^\gamma}$) vicinal coupling constants using the following equations[31-33]:

$$^3J_{H^\alpha H^\beta} = P \cdot {}^{ap}J_{H^\alpha H^\beta} + (1 - P) \cdot {}^{sc}J_{H^\alpha H^\beta};$$

$$^3J_{H^\alpha C^\gamma} = P' \cdot {}^{ap}J_{H^\alpha C^\gamma} + (1 - P') \cdot {}^{sc}J_{H^\alpha C^\gamma}$$

where P and P' are rotamer populations corresponding to the antiperiplanar (ap) arrangements of the relevant spins. The following standard values were used for antiperiplanar and synclinal (sc) arrangements of spins[31-33]: $^{ap}J_{H^\alpha H^\beta}$ = 13.6 Hz, $^{sc}J_{H^\alpha H^\beta}$ = 2.6 Hz, $^{ap}J_{H^\alpha C^\gamma}$ = 8.5 Hz, and $^{sc}J_{H^\alpha C^\gamma}$ = 1.4 Hz. An error of ±5% for rotamer pop-

ulations can be estimated from the inaccuracy of the coupling constants.

The low sample concentration did not allow us to measure the heteronuclear long-range coupling constants for peptide II. The ^{13}C chemical shift of the β-methyl carbon of Phe[4] can be used, however, as a sensitive measure of side-chain conformation, taking advantage of the conformational dependence of γ-substituent effect.[34,35] The contributions of the NH and CO substituents to the β-methyl ^{13}C chemical shifts are given by the following equation:

$$\delta_{\beta\text{-Me}} = \delta_{\text{ref}} + P_{\text{I}} \cdot \delta_{\text{CO}}^{gauche} + P_{\text{II}} \cdot \delta_{\text{NH}}^{gauche} + P_{\text{III}} \cdot \delta_{\text{CO,NH}}^{gauche}$$

where δ_{ref} is the reference β-methyl ^{13}C chemical shift; $\delta_{\text{CO}}^{gauche}$, $\delta_{\text{NH}}^{gauche}$, and $\delta_{\text{CO,NH}}^{gauche}$ are the shielding parameters of the relevant substituents in a *gauche* orientation to the β-methyl carbon (−3.2, −5.1, and −8.3 ppm, respectively[36]), and P_{I}–P_{III} are populations of corresponding staggered rotamers. The δ_{ref} was assumed to be equal for peptides I and II, and its value was calculated from the known β-methyl carbon shift and rotamer populations of peptide I using the above equation.

Energy Calculations

The energy calculations were performed using the Empirical Conformational Energy Program for Peptides (ECEPP/2) force field[37,38] with standard rigid-valence geometry. The β-methyl groups of β-MePhe[4], D-Pen[2], and D-Pen[5] residues were considered as united atomic centers with the United Atom Conformational Energy Program for Peptides (UNICEPP) parameters[39] for nonbonded interactions. Valence geometry of the NO_2 group has been optimized using the Assisted Model Building with Energy Refinement (AMBER) force field[40] for the model benzyl-NO_2 compound, which resulted in a C—N bond length of 1.490 Å, N—O bond lengths of 1.201 Å, C—N—O bond angles of 118.5°, and a O—N—O bond angle of 123.0°. Atomic charges of +0.770 eu at N atom and of −0.433 eu at both O atoms were calculated using Mulliken population analysis as implemented in the MacroModel program.[41] A dielectric constant $\varepsilon = 45$ was used to mimic to some extent the DMSO environment.

Low-energy conformers ($\Delta E = E - E_{\min} \leq 10$ kcal/mol) obtained in a previous study[18] for four stereoisomers of [β-MePhe[4]]DPDPE were considered as initial conformations for the respective stereoisomers of [β-Me-*p*-NO_2Phe[4]]DPDPE. These conformers were energy reminimized after attachment of the *p*-NO_2 group to the phenyl ring of β-MePhe[4]. Initial conformations of the Tyr[1] and β-Me-*p*-NO_2Phe[4] side chains were obtained before energy minimization using the optimization procedure described in reference.[9] Strong parabolic penalty potentials with force constants of 1000 kcal/mol·Å^2 were applied during energy minimization to the interatomic distances S—S and C^β—S in order to maintain standard S—S bond lengths and C^β—S—S bond angles,[37] while a penalty potential of 10 kcal/mol·Å^2 was applied to the C^β—C^β distance to simulate the barrier of rotation around the S—S bond.[37]

For each analogue under study a set of low-energy conformers ($\Delta E \leq 10$ kcal/mol) was selected and classified according to backbone and disulfide bridge conformations. The one-letter code of Zimmerman et al.[42] was used to classify backbone conformations, while disulfide bridge conformations were distinguished by assignment of *trans* ($\chi^1 = 180° \pm 60°$), *gauche* (+; $\chi^1 = 60° \pm 60°$), and *gauche* (−; $\chi^1 = -60° \pm 60°$) rotamers for the side chains of D-Pen[2] and D-Pen[5]. If a group of conformers had common backbone and disulfide bridge conformations, the lowest-energy one was selected to represent this group for comparison with nmr data.

The energy minimization, classification of conformers, and calculation of their parameters related to nmr data were carried out on a cluster of microVAX workstations. Visualization of resulting conformers was performed on a Silicon Graphics Iris 4D/20G+ workstation using the MacroModel V3.6[41] and SYBYL 6.0[43] molecular modeling systems.

Comparison of the NMR and Energy Calculation Data

Expected values of $^3J_{\text{HNC}^\alpha\text{H}}$ coupling constants were calculated from φ torsion angles of low-energy conformers using the Karplus equation with Bystrov parameters.[44] We assumed the value of 2.0 Hz as a reasonable estimate for the standard deviation of calculated $^3J_{\text{HNC}^\alpha\text{H}}$ caused both by an uncertainty in parameterization of the Karplus–Bystrov equation[44] and by φ angle fluctuations within local energy minima. Therefore, conformers, which satisfy inequalities $|J_{\text{calc}} - J_{\text{exp}}| \leq 2.0$ Hz for all calculated $^3J_{\text{HNC}^\alpha\text{H}}$, were assumed to be in agreement with the experimental coupling constants.[45] We have assumed, according to Ref. 20, the upper limits of 2.5, 3.0, and 4.0 Å for the interproton distances corresponding to strong, medium, and weak NOE cross peaks, respectively. Two alternatives of stereospecific assignment were considered for a pair of methylene protons with nonoverlapping resonances, while the shorter of two distances to a pair of overlapping methylene protons was compared with the corresponding NOE. Methyl protons were represented by a central carbon atom, the corresponding upper distance limits being extended by 1.0 Å for each methyl group.

RESULTS

NMR Data

Proton nmr data, including chemical shifts, coupling constants, and temperature coefficients of amide protons measured for three stereoisomers of

Table I ^{1}H Chemical Shifts (δ in ppm) and Coupling Constants (J in Hz) for Analogues I–III (T = 310 K, DMSO-d_6)[a]

	NH			H^α			H^β			H^γ		
Residue	I	II	III	I	II	III	I	II	III	I	II	III
Tyr[1]				4.27 $J_{\alpha\beta}$ = 6.9 $J_{\alpha\beta'}$ = 8.2	4.29 $J_{\alpha\beta}$ = 6.6 $J_{\alpha\beta'}$ = 8.4	4.15 $J_{\alpha\beta}$ = 7.6 $J_{\alpha\beta'}$ = 7.6	2.94 β 2.79 β' $J_{\beta\beta'}$ = 14.0	2.95 β 2.79 β' $J_{\beta\beta'}$ = 14.0	2.89 β 2.84 β' $J_{\beta\beta'}$ = 14.0			
D-Pen[2]	8.46 $J_{NH\alpha}$ = 9.2 (5.2)	8.62 $J_{NH\alpha}$ = 9.0 (3.4)	8.53 $J_{NH\alpha}$ = 9.0 (5.1)	4.48	4.56	4.23				1.18 γ 1.01 γ'	1.24 γ 1.03 γ'	1.05 γ 0.97 γ'
Gly[3]	8.46 $J_{NH\alpha}$ = 9.1 $J_{NH\alpha'}$ = 1.2 (4.6)	8.62 $J_{NH\alpha}$ = 8.0 $J_{NH\alpha'}$ = 0.7 (3.6)	8.41 $J_{NH\alpha}$ = 5.9 $J_{NH\alpha'}$ = 6.8 (1.9)	4.14 α 3.11 α' $J_{\alpha\alpha'}$ = 14.1	4.45 α 3.25 α' $J_{\alpha\alpha'}$ = 14.6	3.67 α 3.53 α' $J_{\alpha\alpha'}$ = 15.4						
β-Me-Phe[4]	8.33 $J_{NH\alpha}$ = 8.6 (5.3)	8.59 $J_{NH\alpha}$ = 8.7 (6.4)	7.54 $J_{NH\alpha}$ = 9.6 (4.7)	4.32 $J_{\alpha\beta}$ = 9.5	4.44 $J_{\alpha\beta}$ = 6.3	4.75 $J_{\alpha\beta}$ = 8.6	3.44 $J_{\beta\gamma}$ = 7.0	3.57 $J_{\beta\gamma}$ = 6.9	3.50 $J_{\beta\gamma}$ = 7.5	1.19	1.29	1.22
D-Pen[5]	7.43 $J_{NH\alpha}$ = 7.8 (2.2)	7.32 $J_{NH\alpha}$ = 8.1 (0.0)	7.71 $J_{NH\alpha}$ = 8.5 (6.6)	4.21	4.25	4.35				1.32 γ 1.32 γ'	1.32 γ 1.29 γ'	1.24 γ 1.21 γ'

[a] Chemical shifts of Tyr and β-Me-Phe aromatic protons are 6.69/7.09 ppm, and 7.54/8.13 ppm, respectively. Temperature coefficients of NH protons (−ppb/K) are given in parentheses.

Table II ^{13}C-NMR Data for Analogues I, II and III (T = 310 K, DMSO-d_6, δ in ppm)[a]

	C^α			C^β			C^γ		
Residue	I	II	III	I	II	III	I	II	III
Tyr^1	53.4	53.2	53.5	36.6	36.2	36.4			
D-Pen^2	59.1	58.8	60.4	51.9	[b]	51.5	25.3	24.8	22.7
							27.3	27.6	27.2
Gly^3	42.5	42.3	42.5						
β-Me-Phe^4	60.1	59.1	56.7	40.4	40.3	40.1	17.9	14.9	17.6
							(1.3)		(1.9)
D-Pen^5	61.8	62.5	61.8	50.5	[b]	50.6	24.5	25.0	22.9
							27.2	27.1	26.4

[a] Chemical shifts of Tyr^1 and β-Me-Phe^4 aromatic carbons are 115.4/130.5 ppm and 123.2/129.0, respectively. The long-range $J_{H^\alpha C^\gamma}$ proton–carbon coupling constants (Hz) for analogues **I** and **III** are given in parentheses.

[b] Nonprotonated β-carbons of D-Pen^2 and D-Pen^5 were not assigned because of the low sample concentration of analogue II (See Methods).

[β-Me-*p*-NO_2Phe^4]DPDPE in DMSO-d_6 are summarized in Table I. ^{13}C chemical shifts obtained for peptides I–III and long-range heteronuclear coupling constants $^3J_{H^\alpha C^\gamma}$ measured for analogues I and III are given in Table II. ROE cross peaks observed for peptides I–III and classified according to their relative intensities[20] are listed in Table III.

Several nmr parameters indicate that the L-Phe^4-containing analogues I and II have a similar well-defined backbone conformation in DMSO. Extremely large differences both in chemical shifts and in $^3J_{HNC^\alpha H}$ coupling constants observed for the two diastereotropic α protons of Gly^3 suggest a highly restricted conformation of the Gly^3 residue.

Table III NOEs Observed for Three Stereoisomers of [β-Me-*p*-NO_2Phe^4]DPDPE

From		To		NOE Intensities[b]		
Residue	Proton[a]	Residue	Proton[a]	2*S*,3*S*	2*S*,3*R*	2*R*,3*R*
Tyr^1	αH	D-Pen^2	NH	s	m	s
D-Pen^2	αH	D-Pen^2	NH	w	w	w
D-Pen^2	αH	Gly^3	NH	s	s	s
D-Pen^2	αH	D-Pen^2	γ	m	m	m
D-Pen^2	αH	D-Pen^2	γ′	w	m	m
D-Pen^2	NH	D-Pen^2	γ	m	m	m
D-Pen^2	NH	D-Pen^2	γ′	m	w	
Gly^3	αH	Gly^3	NH		m[c]	w
Gly^3	α′H	Gly^3	NH	w	w	w
Gly^3	αH	Phe^4	NH	m	m[c]	w
Gly^3	NH	Phe^4	NH			w
Phe^4	αH	Phe^4	NH	w	m[c]	
Phe^4	αH	D-Pen^5	NH			s
Phe^4	αH	Phe^4	β-Me	w	m	m
Phe^4	NH	Phe^4	β-Me		m	
Phe^4	NH	Phe^4	βH	m	w	
Phe^4	NH	D-Pen^5	NH	m	w	
D-Pen^5	αH	D-Pen^5	NH	w	w	m
D-Pen^5	αH	D-Pen^5	γ,γ′	m	m	m

[a] High-field α protons of Gly^3 and γ-methyl protons of D-Pen^{2,5} are denoted as α′ and γ′, respectively.

[b] NOE cross-peak intensities are qualitatively classified as strong (s), medium (m), and weak (w).

[c] These cross peaks are overlapped.

The very small $^3J_{HNC^\alpha H}$ values observed for the high-field α' proton of Gly^3 in analogues I and II, and the large $^3J_{HNC^\alpha H}$ values observed for the low-field α proton are consistent with two narrow regions of ϕ torsion angles around $\pm 150°$.[44] The low-field shift observed for the α proton can be explained by the strong anisotropy effect[46] of the closely spaced carbonyl group of D-Pen^2. Note that a chemical shift difference of ca. 1.20 ppm between two α protons of Gly^3 also has been observed for DPDPE both in DMSO and in water.[2,3,18] However, the $^3J_{HNC^\alpha H}$ coupling constants measured for the Gly^3 residues of DPDPE,[2,3,18] and of the (2S, 3S)- and (2S, 3R)-stereoisomers of [β-MePhe^4]DPDPE[18] were not so extremely distinct as those found for analogues I and II in the present study. This comparison suggests that a more restricted or slightly biased conformation of Gly^3 can appear upon β-Me-p-NO_2 substitution in the L-Phe^4 residue. Low temperature coefficients of the D-Pen^5 NH protons of analogues I and II, an NOE between NH protons of β-Me-p-NO_2Phe^4 and D-Pen^5, and the absence of a detectable NOE between $C^\alpha H$ of β-Me-p-NO_2Phe^4 and NH of D-Pen^5 also are indicative of a restrained conformation of the disulfide ring in the (2S, 3S)- and (2S, 3R)-stereoisomers of [β-Me-p-NO_2Phe^4]DPDPE.

In contrast, small differences between α-proton chemical shifts and close values of $^3J_{HNC^\alpha H}$ coupling constants observed for the Gly^3 residue of the (2R, 3R)-stereoisomer may indicate either higher conformational mobility of this residue, which results in similar time-averaged nmr parameters of two α protons, or a single favorable conformation with the ϕ angle of Gly^3 about $\pm 90°$.[44] Several other ^{1}H-nmr parameters, including a strong NOE between $C^\alpha H$ of β-Me-p-NO_2Phe^4 and NH of D-Pen^5, an NOE between NH protons of Gly^3 and β-Me-p-NO_2Phe^4, a high temperature coefficient of the D-Pen^5 NH, and a low temperature coefficient of the Gly^3 NH indicate a different solution conformation of the 14-membered disulfide ring of the D-Phe^4-containing analogue III in comparison with the two L-Phe^4-containing analogues I and II.

Probable Solution Conformations of Peptide Backbone

The energy calculations revealed 26, 27, and 26 conformers of analogues I, II, and III, respectively, which differed either in backbone or in disulfide bridge conformation and satisfied an energy cutoff $\Delta E \leq 10$ kcal/mol. Comparing these conformers with the nmr data, we first searched for structures that satisfy all $^3J_{HNC^\alpha H}$ coupling constants for residues 3–5, and all distance constraints between backbone $C^\alpha H$ and NH protons in the cyclic parts of the molecules. The backbone conformers selected at this stage for analogues I, II, and III are listed in Table IVa, b, and c, respectively, which also contain $^3J_{HNC^\alpha H}$ coupling constants and interproton distances predicted by these conformers. For comparison, Table IV also includes the lowest energy conformers (1) of all three analogues and the conformers (2) of analogues I and II, which are close in backbone structure to the biologically active conformations of DPDPE proposed elsewhere.[9] As a second step, we eliminated those conformers that were in major disagreement with nmr data for the acyclic parts of the molecules. Finally, we compared interproton distances of selected conformers with the complete set of observed NOEs in order to confirm their relevance as possible solution conformations and to check them for a consistency with side-chain-related NOEs. Backbone and disulfide bridge torsion angles of the most probable solution conformations of analogues I–III are given in Table V.

The energy minimization of [(2R, 3S)-β-Me-p-NO_2Phe^4]DPDPE (analogue IV) resulted in 24 low-energy conformations. Although analogue IV was not available for a comprehensive nmr study, relative energies of its representative conformers are included it Table IVc (in parentheses) for comparison with the respective conformations of analogue III. Generally, the (2R, 3R)- and (2R, 3S)-stereoisomers have very similar backbone conformations and differ by the favorable χ^1 rotamers of the β-Me-p-NO_2Phe^4 side chains.

[(2S, 3S)-β-Me-p-NO$_2$Phe^4]DPDPE (I). Conformers 3–8 in Table IVa predict $^3J_{HNC^\alpha H}$ coupling constants of Gly^3 and Phe^4 close to the experimental values, and $^3J_{HNC^\alpha H}$ of D-Pen^5 at the upper boundary of the accepted ± 2.0 Hz deviation from the experimental value. Discussing nmr data we concluded that ϕ angle of the Gly^3 residue in analogues I and II should belong to one of the two narrow symmetric regions around $\pm 150°$. Conformers 3–8 have positive ϕ angles about 150°. This allows stereospecific assignment of *pro-S* and *pro-R* configuration to the low-field α proton and high-field α' proton of Gly^3, respectively. Interproton distances predicted by conformers 3–8 are in agreement with nuclear Overhauser effects (NOEs) observed between backbone protons of analogue I. Moreover, in the ROESY spectrum of analogue I (Figure 2), no cross peak was detected for the sequential pairs

Table IV Comparison of Low-Energy Conformers of Three Stereoisomers of [β-Me-*p*-NO_2Phe^4]DPDPE with ^{1}H-NMR Data

Backbone Conformer[a]	ΔE[b] (kcal/mol)	$^3J_{HNC^\alpha H}$ (Hz,[c] Residue No.)					NOE[d] and Interproton Distances, Å: $C^\alpha H_i - NH_{i+1}$, i =					$NH_i - NH_{i+1}$, i =	
			3[e]		4	5	1	2	3[e]		4		
		2	*pro-R*	*pro-S*					*pro-R*	*pro-S*		3	4
a. (2*S*,3*S*)-Stereoisomer, Experimental Data		**9.2**	**1.2**	**9.1**	**8.6**	**7.8**	**s**	**s**	**no**	**m**	**no**	**no**	**m**
1. *E E*C*A E**	0.0	9.4	7.2	6.8	5.6	9.7	2.3	2.3	3.7	2.7	3.6	3.6	2.6
2. *E F*B*G E**	2.7	6.0	6.7	7.5	9.1	9.7	2.3	2.4	3.3	3.4	3.6	2.5	2.2
3. *E F*D*G E**	3.1	3.8	0.4	7.8	10.0	9.8	2.3	2.3	3.6	2.7	3.6	4.0	2.5
4. *A E*D*A E**	3.5	9.5	0.4	8.5	9.5	9.9	3.6	2.3	3.6	2.6	3.6	3.6	2.6
5. *E E*D*A E**	4.6	9.1	0.4	8.2	9.6	9.9	2.4	2.3	3.6	2.6	3.6	4.2	2.3
6. *A*E*D*A E**	5.3	9.1	0.4	8.2	9.4	9.9	3.1	2.3	3.6	2.6	3.6	4.0	2.3
7. *A*F*D*G E**	6.0	4.3	0.4	7.8	10.0	9.8	3.1	2.3	3.7	2.7	3.6	4.0	2.2
8. *E E*D*G E**	8.6	8.6	0.7	9.8	9.1	10.0	2.2	2.2	3.6	3.0	3.6	4.3	2.2
b. (2*S*,3*R*)-Stereoisomer, Experimental Data		**9.0**	**0.7**	**8.0**	**8.7**	**8.1**	**m**	**s**	**no**	**ov**[f]	**no**	**ov**[f]	**w**
1. *E E*C*A E**	0.0	9.5	7.3	6.7	4.7	9.7	2.3	2.3	3.6	2.6	3.6	3.7	2.7
2. *E F*B*G E**	3.6	5.9	7.5	6.3	8.8	9.7	2.3	2.4	3.3	3.4	3.6	2.5	2.3
3. *E F*D*A E**	2.8	3.8	0.4	8.4	8.7	9.8	2.3	2.3	3.6	2.6	3.6	4.2	2.5
4. *A E*D*A E**	3.0	9.5	0.4	9.1	8.1	9.9	3.6	2.2	3.6	2.5	3.6	4.4	2.5
5. *E E*D*A E**	4.2	9.0	0.4	8.6	8.5	9.8	2.4	2.3	3.6	2.5	3.6	4.3	2.5
6. *A*E*D*A E**	4.8	9.1	0.4	8.9	8.0	9.9	3.1	2.3	3.6	2.5	3.6	4.3	2.6
7. *A*F*D*A E**	5.7	4.1	0.4	8.4	8.6	9.8	3.1	2.3	3.6	2.6	3.6	4.2	2.5
8. *E E*D*G E**	9.0	8.6	0.6	9.6	9.8	10.0	2.2	2.2	3.6	2.9	3.6	4.3	2.2
9. *A E*D*G E**	9.8	8.7	0.8	10.0	9.7	10.0	3.6	2.2	3.6	2.9	3.6	4.4	2.2
c. (2*R*,3*R*)-Stereoisomer, Experimental Data		**9.0**	**5.9**	**6.8**	**9.6**	**8.5**	**s**	**s**	**w**	**ov**[f]	**s**	**w**	**no**
1. *E A*A A E**	0.0 (0.0)	5.6	7.5	6.7	8.0	9.6	2.3	3.5	3.6	2.9	2.4	2.4	3.2
2. *A E*A*D*E**	1.5 (1.7)	9.2	6.5	7.8	9.3	9.0	3.6	2.2	2.6	3.6	2.2	2.6	3.9
3. *E E*A*D*E**	2.4 (2.7)	8.7	6.3	8.1	9.3	9.0	2.4	2.2	2.6	3.6	2.2	2.5	3.8
4. *A*E*A*D*E**	3.1 (3.4)	8.8	6.3	8.1	9.3	9.0	3.0	2.2	2.6	3.6	2.2	2.5	3.9
5. *E E*A*D*E**	8.4 (8.6)	8.9	6.0	8.4	9.2	9.7	2.4	2.3	2.6	3.6	2.2	2.6	3.9

[a] The one-letter code of Zimmerman et al.[42] is used to denote the backbone conformation of each amino acid residue.

[b] Relative energies $\Delta E = E - E_{min}$ for conformers of analogues I–III. Relative energies for analogue IV are given in parentheses under the energies of respective conformers of analogue IV.

[c] Expected values of $^3J_{HNC^\alpha H}$ coupling constants were calculated from torsion angles ϕ of low-energy conformers using the Karplus–Bystrov equation.[44]

[d] Intensities of cross peaks in ROESY spectra were qualitatively classified into the following grades: **s,** strong; **m,** medium; **w,** weak; **no,** no detectable NOE was observed.

[e] Experimental $^3J_{HNC^\alpha H}$ coupling constants and NOE cross peaks are assigned to *pro-R* and *pro-S* α protons of the Gly^3 residues, so as to achieve the best agreement with corresponding parameters of low-energy conformers. For the (2*R*,3*R*)-stereoisomer the assignment is tentative.

[f] NOE cross peak cannot be definitely detected or assigned due to a resonance overlap.

Table V Backbone and Disulfide Bridge Torsion Angles of Probable Solution Conformations of Three Stereoisomers of [β-Me-*p*-NO_2Phe^4]DPDPE

		Stereoisomer, Conformers						
		2*S*,3*S*		2*S*,3*R*			2*R*,3*R*	
Residue	Angle	**5**	**8**	**5**	**6**	**8**	**3**	**5**
Tyr^1	ψ	161	120	161	25	120	161	154
	ω	179	179	178	180	179	178	−175
D-Pen^2	ϕ	138	143	139	138	143	142	140
	ψ	−136	−125	−135	−134	−126	−130	−122
	ω	−174	−164	−172	−172	−164	−169	−152
	χ^1	−171	88	−170	−171	89	−164	81
	χ^2	−124	114	−127	−124	113	−159	124
Gly^3	ϕ	149	135	146	144	138	90	92
	ψ	−62	−34	−70	−72	−39	62	62
	ω	174	177	172	173	171	180	−171
β-MePhe^4	ϕ	−108	−138	−96	−92	−129	136	137
	ψ	−59	−59	−66	−66	−62	−98	−102
	ω	178	175	−178	180	179	−178	179
D-Pen^5	ϕ	126	117	128	126	122	139	131
	ψ	−150	−147	−146	−147	−146	−140	−148
	χ^1	−68	−65	−65	−66	−64	−56	−66
	χ^2	88	153	87	88	154	85	147
$\angle C^\beta$-S-S-C^β		109	−108	109	110	−109	121	−105

of protons Gly^3 $C^{\alpha'}H$ - Phe^4 NH, Gly^3 NH–Phe^4 NH, and Phe^4 $C^\alpha H$ - D-Pen^5 NH. All distances predicted for these pairs of protons in conformers 3–8 are longer than 3.5 Å, which validates the upper limit distances applied in this study. Conformers 3–8 possess a similar backbone conformation of the 14-membered disulfide ring and differ mainly in the torsion angles ψ of Tyr^1 and ϕ of D-Pen^2. The nmr data related to these torsion angles allow us to exclude several conformers of the N-terminal part of the (2S, 3S)-stereoisomer I. Thus, conformers 3 and 7 are incompatible with the $^3J_{HNC^\alpha H}$ coupling constant of D-Pen^2, while conformers 4 and 6 violate the distance constraint imposed by the strong NOE between the Tyr^1 $C^\alpha H$ and the D-Pen^2 NH. The conformers 5 and 8 satisfy all the nmr data considered in Table IVa and, therefore, we conclude that these conformers represent the most probable backbone conformation of analogue I in DMSO. Superimposed stereoviews of conformers 5 and 8 are shown in Figure 4.

Conformer 5 has a right-handed disulfide bridge with the dihedral angle $C^\beta—S—S—C^\beta \approx 110°$ and a *trans* rotamer for the D-Pen^2 χ^1, while the conformer 8 has a left-handed disulfide bridge with the angle $C^\beta—S—S—C^\beta \approx -110°$ and a *gauche* (+) rotamer for the D-Pen^2 χ^1. Generally, the χ^1 rotamers of D-Pen^2 can be distinguished by the relative intensities of NOEs between $C^\alpha H$, NH, and γ-methyl protons of D-Pen^2. The γ- and γ′-methyl resonances of the (2S, 3S)-stereoisomer are well separated and give, respectively, medium and weak NOEs with $C^\alpha H$, and two similar medium-intensity NOEs with NH of D-Pen^2 (see Table III). Both conformers predict $H^\alpha—C^\gamma$ distances of 3.0 ± 0.4

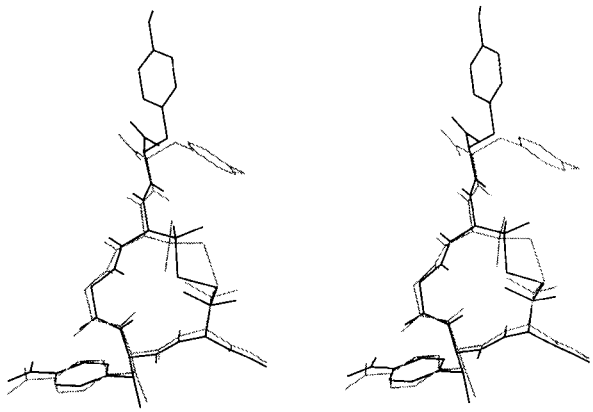

FIGURE 4 Superposition of the probable solution conformations of [(2S, 3S)-β-Me-*p*-NO_2Phe^4]DPDPE with right-handed (bold line) and left-handed (shadow line) conformations of the disulfide bridge.

Å, which are consistent with corresponding NOEs. However, each conformer predicts one short (2.8 Å) and one long (about 4.0 Å) distance between the NH proton and the *two different* γ-carbons of D-Pen^2. This pattern is not consistent with the two medium-intensity NOEs, unless one assumes an equilibrium between *trans* and *gauche* (+) rotamers of the D-Pen^2 residue represented by conformers 5 and 8, respectively. Therefore, we conclude that both right-handed and left-handed conformers of the disulfide bridge can exist in DMSO in a dynamic equilibrium.

[(2S, 3R)-β-Me-p-NO$_2$Phe^4]DPDPE (II). Low-energy conformers 3–9 of analogue II (Table IVb) satisfying the nmr constraints for residues 3–5 have similar backbone conformations of the cyclic part of the molecule. As for analogue I, nmr data on the acyclic part of analogue II allow us to exclude conformers 3 and 7, which predict too small $^3J_{HNC^\alpha H}$ values for D-Pen^2, and conformers 4 and 9, which are inconsistent with the medium-intensity NOE between the C$^\alpha$H of Tyr^1 and NH of D-Pen^2. Conformers 5, 6, and 8 of Table IVb satisfy all available nmr data and may be considered as the most probable solution conformations for the (2S, 3R)-stereoisomer II in DMSO. Two of them (conformers 5 and 8) are very close to the probable solution conformers selected for the (2S, 3S)-stereoisomer, and possess, respectively, right-handed and left-handed conformations of the disulfide bridge. For the (2S, 3R)-stereoisomer the NOEs observed between the NH and the two γ-methyl protons of D-Pen^2 differ in intensities (medium and weak, see Table III), and they are compatible both with *trans* and with *gauche* (+) rotamers of the χ^1 angle of D-Pen^2. Therefore, in contrast with the (2S, 3S)-stereoisomer I, the NOE pattern observed for the (2S, 3R)-stereoisomer II does not require the assumption of an equilibrium between two conformers of the disulfide bridge, although it does not allow us to discriminate which of the two conformers is preferred. Conformer 6 differs from conformer 5 only in the ψ angle of Tyr^1. The similar conformer of analogue I has been excluded as incompatible with a strong NOE between the C$^\alpha$H of Tyr^1 and the NH of D-Pen^2. The medium NOE observed for analogue II is consistent with an equilibrium between conformers 5 and 6 in DMSO. This may either reflect real difference in mobility of the Tyr^1 residue in analogues I and II, or be attributed to an inadequacy of the qualitative classification of NOE intensities.

[(2R, 3R)-β-Me-p-NO$_2$Phe^4]DPDPE (III). Four low-energy conformers were found to satisfy the NOE constraints and the $^3J_{HNC^\alpha H}$ coupling constants for residues 3–5 of the analogue (conformers 2–5 in Table IVc). A strong NOE between the Tyr^1 C$^\alpha$H and the D-Pen^2 NH allowed us to exclude conformers 2 and 4 with negative and small positive values of the Tyr^1 ψ angle, respectively. Thus, only conformers 3 and 5, which are in agreement with all backbone NOEs and coupling constants, can be considered as the most probable solution conformations of the (2R, 3R)-stereoisomer III in DMSO.

Conformers 3 and 5 have similar backbone conformations, but differ in the disulfide bridge conformation. As for analogues I and II, the lower energy conformer 3 has a right-handed disulfide bridge with the dihedral angle $C^\beta—S—S—C^\beta \approx 120°$ and a *trans* rotamer for the D-Pen^2 χ^1, while conformer 5 has a left-handed disulfide bridge with the angle $C^\beta—S—S—C^\beta \approx -105°$ and a *gauche* (+) rotamer for the D-Pen^2 χ^1. Two medium-intensity NOEs observed between the C$^\alpha$H and γ-methyl protons of D-Pen^2 and only one NOE observed between the NH and γ-methyl protons of D-Pen^2 (see Table III) are consistent with the $H^\alpha—C^\gamma$ distances of 3.0 ± 0.4 Å and the $NH—C^\gamma$ distances of 2.8 Å and about 4.0 Å predicted by *either* of the two χ^1 rotamers. Therefore, the NOE pattern is consistent with either of the two conformers of the disulfide bridge and does not require an assumption of a dynamic equilibrium between them.

Rotamer Populations of the Tyr^1 and β-Me-*p*-NO$_2$Phe^4 Side Chains

Determination of the χ^1 rotamer population for β-MePhe^4 was not a trivial problem, because only one homonuclear $^3J_{H^\alpha H^\beta}$ coupling constant was available for this residue. For peptides I and III, heteronuclear $^3J_{H^\alpha C^\gamma}$ coupling constants were employed for calculation of the β-Me-*p*-NO$_2$Phe^4 rotamer populations as described in Methods. Limited amounts of peptide II did not allow us to measure the heteronuclear long-range coupling constants. In this case we used the conformational dependence of the β-methyl ^{13}C chemical shift,[34,35] which was calibrated using χ^1 rotamer populations previously determined for analogue I. The resulting rotamer populations for the β-Me-*p*-NO$_2$Phe^4, as well as rotamer populations for Tyr^1 determined by Pachler's analysis,[32] are given in Table VI. Rotamer populations found for the Tyr^1 and Phe^4

Table VI Rotamer Populations of the Tyr[1] and Phe[4] Side Chains for DPDPE and [β-Me-*p*-NO_2Phe[4]]DPDPE in DMSO

	Rotamer Populations, %					
	Tyr[1]			Phe[4]		
Peptides	P(g^-)	P(t)	P(g^+)	P(g^-)	P(t)	P(g^+)
DPDPE[a]	39	60	1	69	17	14
I	51	39	10	63	0	37
II	53	36	11	60	34	6
III	45	45	10	39	7	54

[a] Data for DPDPE in DMSO were taken from Ref. 3.

side chains of DPDPE in DMSO[3] are included in Table VI for comparison.

DISCUSSION

β-Methyl derivatives of aromatic amino acids initially were designed as a tool to stabilize one of χ^1 rotamers with respect to two other rotamers, depending on the chiralities at the C^α and C^β positions of the β-methyl-substituted residue. The rotamer populations found in this study for the three stereoisomers of [β-Me-*p*-NO_2Phe[4]]DPDPE, and the almost identical populations obtained earlier for the stereoisomers of [β-MePhe[3]]cholecystokinin-8[47] revealed a more complicated rotamer equilibrium for the β-methyl substituted side chains. Introduction of the second bulky substituent at the β position of phenylalanine does not stabilize one particular χ^1 rotamer, but it discriminates the χ^1 rotamer that places both β-substituents in a *gauche* orientation to the carbonyl group of the same residue, i.e., a *trans* rotamer for both *erythro*-isomers (2S, 3S) and (2R, 3R) of β-MePhe, a *gauche* (+) rotamer for the (2S, 3R)-stereoisomer, and a *gauche* (−) rotamer for the (2R, 3S)-stereoisomer (see Ref. 47). The two other rotamers become almost equally populated upon β-methyl substitution. Therefore, this substitution is a useful tool to discriminate a particular rotamer for an aromatic side chain in order to examine, if this rotamer is the one responsible for biological activity. For example, all three rotamers of the Phe[4] side chain of DPDPE are populated in water and in DMSO.[3] In contrast, for [(2S, 3S)-β-Me-*p*-NO_2Phe[4]]DPDPE, which is almost as active as DPDPE in the δ-opioid receptor bioassay,[16] the population of the *trans* rotamer approaches zero. If we assume the discrimination from the *trans* rotamer to be a steric property of the (2S, 3S)-β-MePhe side chain, independent of the environment, we can conclude that the *trans* rotamer of Phe[4] is irrelevant to the δ-receptor activity of DPDPE. Moreover, the most active (2S, 3S)- and (2S, 3R)-stereoisomers of [β-Me-*p*-NO_2Phe[4]]-DPDPE (see Ref. 16) have only one common, highly populated rotamer of Phe[4], the *gauche* (−) rotamer. Therefore, based on the results of this study, the *gauche* (−) rotamer may be suggested as the probable rotamer of the Phe[4] side chain in the δ-receptor-bound state of DPDPE and its active analogs.

As a result of the combined nmr and molecular mechanics study, a small number of low-energy conformers have been selected as probable solution conformations for each of the three stereoisomers of [β-Me-*p*-NO_2Phe[4]]DPDPE. It is interesting to compare the probable solution conformations proposed for the β-methylated analogues in this and previous[18] studies, and with the models for the solution conformation of DPDPE suggested earlier.[2,3,18] Furthermore, comparison of the solution conformations proposed here with the crystal structure of DPDPE[14] and the models of the biologically active conformations[9] can shed light on relationships between conformations of DPDPE analogues in different environments and in the receptor-bound state. Comparisons of pairs of conformers were performed by best-fit spatial matching[48] of all C^α and C^β atoms.

Comparison of the torsion angles in Table V reveals that the (2S, 3S)- and (2S, 3R)-stereoisomers I and II have very similar backbone conformations in DMSO. The same *gauche* (−) rotamer of the β-Me-*p*-NO_2Phe[4] side chain was found to be most populated for both analogues. Although minor

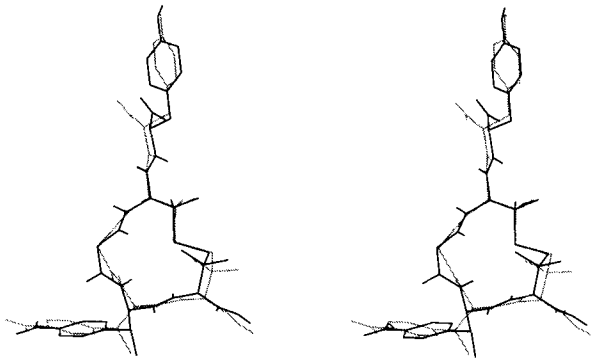

FIGURE 5 Superposition of the probable solution conformations of (2S, 3S)-stereoisomer with a *gauche* (−) rotamer of Phe[4] (bold line) and (2R, 3R)-stereoisomer with a *gauche* (+) rotamer of Phe[4] (shadow line).

differences in the conformational mobilities of the Tyr[1] residue and the disulfide bridge moieties in these two analogues could not be excluded with the available nmr data, the conformational similarity of analogues I and II allows us to consider the lower energy conformer 5 of analogue I (Tables IV and V) as representative of the solution conformation of both analogues. We will denote this conformation as conformer **S**. By analogous considerations, we will assume conformer 3 of analogue III as representative of the solution conformation of this analogue and denote it as conformer **R**.

Superposition of conformers **S** and **R** shown in Figure 5 reveals a similar backbone shape for the L- and D-Phe[4]-containing analogues with rms deviation of 0.64 Å for all C^{α} and C^{β} atoms. Such a close similarity could not be inferred either from the substantially different nmr parameters or from the different sets of backbone torsion angles of the probable solution conformers of the (2S, 3S)- and (2R, 3R)-stereoisomers (see Table V). However, the difference in torsion angles results mainly in a rotation of the plane of the peptide group between Gly[3] and β-Me-*p*-NO_2Phe[4] by about 120°, and in an additional rotation of the ϕ angle of Gly[3] by about 60°. These local conformational differences allow the structures to accommodate both L- and D-Phe[4] within the same overall backbone shape, while different spatial positions of the $C^{\alpha}H$ and NH protons of L- and D-Phe[4] result in different patterns of NOE. The difference of 60° in the ϕ angle of Gly[3] is the reason for the considerably different $^3J_{HNC^{\alpha}H}$ coupling constants observed for this residue in the two stereoisomers. With the most populated χ^1 rotamers of β-Me-*p*-NO_2Phe[4] [*gauche* (−) for analogue I and *gauche* (+) for analogue III], the α-amino groups and the aromatic rings of Tyr[1] and Phe[4] of analogues I and III in the proposed solution conformations can overlap almost completely (see Figure 5).

Solution conformations of the four stereoisomers of [β-MePhe[4]]DPDPE have been proposed in a previous study[18] utilizing a comparison of low-energy conformers with experimental coupling constants $^3J_{HNC^{\alpha}H}$. Conformer **S** found in the present study matches conformer 10 of [(2S, 3S)-β-MePhe[4]]DPDPE (Table III in Ref. 18) with an rms = 0.43 Å. A good match was found also for conformer **R** and conformer 10 (Table 3 in Ref. 18) of [(2R, 3R)-β-MePhe[4]]DPDPE (rms = 0.47 Å). Therefore, it may be concluded that similar conformers of [β-MePhe[4]]DPDPE and [β-Me-*p*-NO_2Phe[4]]DPDPE contribute to their solution equilibria in DMSO. On the other hand, comparison of the $^3J_{HNC^{\alpha}H}$ coupling constants observed for the (2S, 3S)- and (2S, 3R)-stereoisomers in the previous[18] and the present studies allows us to suggest that the polar NO_2 group restricts further the conformational mobility of these stereoisomers in solution.

Table VII lists the results of comparison of conformers **S** and **R** with several models of DPDPE conformations proposed by various authors.[2,3,9,14,18] The first two columns of Table VII relate to two types of conformers that were suggested for DPDPE in water (conformers 4 and 20 in Table 3 of Ref. 18); the first of them was assumed to be retained in DMSO. The next two columns correspond to solution conformations of DPDPE derived from nmr studies and subsequent energy calculations by Hruby et al. (conformer 2′ in Ref. 2) and by Mosberg et al. (conformer III′ in Ref. 3). Then, three columns display results of comparison of conformers **S** and **R** to the three crystal structures of DPDPE revealed by the x-ray analysis (conformers 1–3 in Table 2 of Ref. 14). Finally, conformers **S** and **R** were compared to the "biologically active" conformations (BAC) of DPDPE, proposed recently as a result of extensive conformation–activity studies of linear and cyclic δ-selective opioid peptides (conformers 1–3 in Table VII of Ref. 9). The rms values in the upper parts of each entry of Table VII correspond to comparison of entire molecules, and those in the lower parts correspond to comparison of cyclic moieties only.

The data of Table VII show that conformer 20, which was suggested in Ref. 18 as a model for solution structure of DPDPE in water, is, perhaps, the most similar to both conformers **S** and **R**, out of all other models of solution structure of DPDPE. It is noteworthy that the $^3J_{HNC^{\alpha}H}$ values predicted for

Table VII Comparison of Probable Solution Conformations of the (2S,3S)- and (2R,3R)-Stereoisomers of [β-Me-*p*-NO_2Phe^4]DPDPE to Various Models of DPDPE Proposed by Other Authors: RMS Deviations of C^α and C^β Atoms in Å[a]

	Model Type											
	Solution Structure Models					Crystal Structures			BAC Models			
	Ref. 18		Ref. 2	Ref. 3		Ref. 14			Ref. 9			
	Conformer 4	Conformer 20	Conformer 2′	Conformer III′		Conformer 1	Conformer 2	Conformer 3	Conformer 1	Conformer 2	Conformer 3	
S	1.81	0.61	2.40	1.77		2.10	2.87	2.17	2.72	2.67	2.71	
	1.66	0.61	1.22	2.29		2.88	2.92	2.90	1.56	1.58	1.55	
R	1.35	1.02	2.07	1.38		1.82	> 3.0	1.93	2.42	2.35	2.41	
	1.11	1.21	0.89	1.85		2.56	2.61	2.61	0.95	0.97	0.95	

[a] The upper number in each entry is rms deviation of all C^α and C^β atoms, the lower number is rms deviation of C^α and C^β atoms of the cyclic parts of the molecules.

Gly^3 residue by the models of Hruby and Mosberg (ϕ angles about −100° and 80°, respectively) are substantially larger than the very small coupling constant observed for one of the α protons of Gly^3 in analogues I and II. Therefore, none of these two conformers suggested for DPDPE can contribute with a considerable statistical weight to the conformational equilibrium of the (2S, 3S)- and (2S, 3R)-stereoisomers of [β-Me-*p*-NO_2Phe^4]DPDPE in DMSO. Conformers **S** and **R** are nonsimilar to the crystal structures of DPDPE, either. Again, the crystal-like structure (ϕ angle of Gly^3 is about 100°) is not consistent with the small $^3J_{HNC^\alpha H}$ coupling constants observed for analogues I and II, and therefore cannot contribute to the conformational equilibrium of these analogues in DMSO.

The above comparison enables us to conclude that the conformational mobility of the (2S, 3S)- and (2S, 3R)-stereoisomers of [β-Me-*p*-NO_2Phe^4]DPDPE in DMSO is more constrained than that of the parent peptide DPDPE. The diversity of models proposed as solution conformations of DPDPE seems to reflect a complex dynamic equilibrium of DPDPE conformers in solution, which may depend on a particular solvent and experimental conditions. As a result of the β-methyl and *p*-NO_2 substitutions in Phe^4, the solution equilibrium for (2S, 3S)- and (2S, 3R)-stereoisomers of [β-Me-*p*-NO_2Phe^4]DPDPE in DMSO is shifted toward similar well-defined conformations that are completely consistent with the nmr data. This type of structure, however, does not match most of the models proposed for DPDPE in solution, as well as the conformations of DPDPE found in crystal state.[14] The nmr data available for the (2R, 3R)-stereoisomer does not exclude the possibility that other types of conformers can contribute to the solution equilibrium together with the solution structure suggested in this study.

The probable solution conformations of the L- and D-Phe^4-containing analogues are very similar and allow almost complete superposition of the main opioid pharmacophores, i.e., α-amino group and aromatic rings of Tyr^1 and Phe^4, as well as of the substituent β-methyl groups (see Figure 5). On the other hand, the (2R, 3R)-stereoisomer of [β-Me-*p*-NO_2Phe^4]DPDPE is 140 times less active in the mouse vas deferens bioassay, than the (2S, 3S)-stereoisomer, and 50 times less potent in δ-receptor binding assay, than the (2S, 3R)-stereoisomer.[16] The only noticeable difference between solution conformers **S** and **R** is in positions of the Gly^3 carbonyl oxygen and the β-Me-*p*-NO_2Phe^4 amide hydrogen. In principle, rotation of the peptide group between Gly^3 and β-Me-*p*-NO_2Phe^4 may cause a

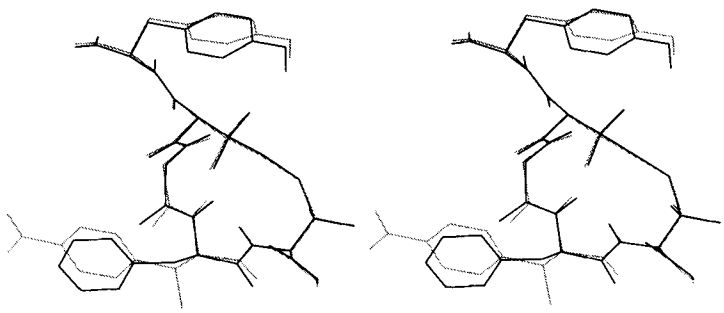

FIGURE 6 Superposition of the BAC of DPDPE (bold line) proposed in Ref. 9 with the most similar low-energy conformations of [(2S, 3S)-β-Me-*p*-NO_2Phe^4]DPDPE (conformer 2 in Table IVa; shadow line).

loss of one or two hydrogen bonds to the receptor, which can explain the 50-fold drop in δ-receptor affinity of the (2R, 3R)-stereoisomer. However, a hydrogen bonding of the Phe^4 amide group to the δ-receptor is not probable, because Phe^4 N-alkylated analogues of enkephalin possess high δ-receptor potencies.[49] Therefore, the contradiction between similar solution conformations and different biological activities of the L- and D-Phe^4-containing stereoisomers suggests that the conformers that are most populated in DMSO may not be relevant to the δ-opioid receptor binding of these analogues.

Comparison of the putative biologically active conformations of DPDPE[9,15] with the solution conformations **S** and **R** revealed their pronounced nonsimilarity, though with a more satisfactory matching of the disulfide ring structures (see Table VII). At the same time, low-energy conformers very close to the BAC of DPDPE were found by energy calculations for the (2S, 3S)- and (2S, 3R)-stereoisomers of [β-Me-*p*-NO_2Phe^4]DPDPE (conformers 2 in Table IVa and b; see also Figure 6). Although these conformers do not satisfy all of the experimental $^3J_{HNC^{\alpha}H}$ values, and, hence, cannot possess a considerable statistical weight in DMSO, they may be favorable in another environment, for example, at the binding site of the δ-opioid receptor. In contrast, no conformer close to the BAC of DPDPE was found for the D-Phe^4-containing analogues III and IV. Energy minimization of these two analogues starting from the BAC model has converged to the solution conformer **R**.

In summary, we can conclude that the model of BAC proposed earlier[9] for DPDPE correlates with the biological activity data on the β-Me-*p*-NO_2Phe^4-substituted analogues of DPDPE better than their solution conformations found in this study. Therefore, the BAC may be considered as tentative models of δ-receptor-bound conformations for the (2S, 3S)- and (2S, 3R)-stereoisomers of [β-Me-*p*-NO_2Phe^4]DPDPE. The contradiction between solution conformations and structure–activity relationships of the β-Me-*p*-NO_2Phe^4-substituted analogues of DPDPE may serve as a warning against a noncritical acceptance of solution structures of peptides as models for their biologically active conformations.

This publication was supported by U.S. Public Health Service (USPHS) Grant NS-19972 and by National Institute of Drug Abuse (NIDA) Grants DA 06284 and DA 04248. Its contents are solely the responsibility of the authors and do not necessarily represent the official views of the USPHS and NIDA. K. E. Kövér thanks the support of the Hungarian Academy of Sciences through Grant OTKA 1144 and T-014982.

REFERENCES

1. Mosberg, H. I., Hurst, R., Hruby, V. J., Gee, K., Yamamura, H. I., Galligan, J. J. & Burks, T. F. (1983) *Proc. Natl. Acad. Sci. USA* **80,** 5871–5874.
2. Hruby, V. J., Kao, L.-F., Pettitt, B. M. & Karplus, M. (1988) *J. Am. Chem. Soc.* **110,** 3351–3359.
3. Mosberg, H. I., Sobczyk-Kojiro, K., Subramanian, P., Crippen, G. M., Ramalingam, K. & Woodard, R. W. (1990) *J. Am. Chem. Soc.* **112,** 822–829.
4. Keys, C., Payne, P., Amsterdam, P., Toll, L. & Loew, G. (1988) *Mol. Pharmacol.* **33,** 528–536.
5. Nikiforovich, G. V., Balodis, J., Shenderovich, M. D. & Golbraikh, A. A. (1990) *Int. J. Peptide Protein Res.* **36,** 67–78.
6. Froimowitz, M. & Hruby, V. J. (1989) *Int. J. Peptide Protein Res.* **34,** 88–96.
7. Froimowitz, M. (1990) *Biopolymers* **30,** 1011–1025.
8. Chew, C., Villar, H. O. & Loew, G. (1991) *Mol. Pharmacol.* **39,** 502–510.

9. Nikiforovich, G. V., Hruby, V. J., Prakash, O. & Gehrig, C. A. (1991) *Biopolymers* **31,** 941–955.
10. Wilkes, B. C. & Schiller, P. W. (1991) *J. Computer-Aided Mol. Design* **5,** 293–302.
11. Pettitt, B. M., Matsunaga, T., Al-Obeidi, F., Gehrig, C., Hruby, V. J. & Karplus, M. (1991) *Biophys. J.* **60,** 1540–1544.
12. Smith, P. E., Dang, L. X. & Pettitt, B. M. (1991) *J. Am. Chem. Soc.* **113,** 67–73.
13. Chew, C., Villar, H. O. & Loew, G. H. (1993) *Biopolymers* **33,** 647–657.
14. Flippen-Anderson, J. L., Hruby, V. J., Collins, N., Clifford, G. & Cudney, B. (1994) *J. Am. Chem. Soc.* **116,** 7523–7531.
15. Nikiforovich, G. V. & Hruby, V. J. (1990) *Biochem. Biophys. Res. Commun.* **173,** 521–527.
16. Hruby, V. J., Toth, G., Gehrig, C. A., Kao, L.-F., Knapp, R., Lui, G. K., Yamamura, H. I., Kramer, T. H., Davis, P. & Burks, T. F. (1991) *J. Med. Chem.* **34,** 1823–1830.
17. Toth, G., Russell, K. C., Landis, G., Kramer, T. H., Fang, L., Knapp, R., Davis, P., Burks, T. F., Yamamura, H. I. & Hruby, V. J. (1992) *J. Med. Chem.* **35,** 2384–2391.
18. Nikiforovich, G. V., Prakash, O., Gehrig, C. A. & Hruby, V. J. (1993) *Int. J. Peptide Protein Res.* **41,** 347–361.
19. Hruby, V. J., Al-Obeidi, F. & Kazmierski, W. (1990) *Biochem. J.* **268,** 249–262.
20. Wüthrich, K. (1986) *NMR of Proteins and Nucleic Acids,* Wiley, New York.
21. Subramanian, S. & Bax, A. (1987) *J. Magn. Reson.* **71,** 325–330.
22. Rance, M. (1987) *J. Magn. Reson.* **74,** 557–564.
23. Bothner-By, A. A., Stephens, R. L., Lee, J., Warren, C. D. & Jeanloz, R. W. (1984) *J. Am. Chem. Soc.* **106,** 811–813.
24. Bax, A. & Davis, D. G. (1985) *J. Magn. Reson.* **63,** 207–213.
25. Kövér, K. E., Prakash, O. & Hruby, V. J. (1993) *J. Magn. Reson. Ser. A* **103,** 92–96.
26. Kövér, K. E., Prakash, O. & Hruby, V. J. (1993) *Magn. Reson. Chem.* **31,** 231–237.
27. Mueller, L. (1979) *J. Am. Chem. Soc.* **101,** 4481–4484.
28. Kövér, K. E., Prakash, O. & Hruby, V. J. (1992) *J. Magn. Reson.* **99,** 426–432.
29. Bax, A. & Davis, D. G. (1985) *J. Magn. Reson.* **65,** 355–360.
30. Marion, D. & Wüthrich, K. (1983) *Biochem. Biophys. Res. Commun.* **113,** 967–974.
31. Pachler, K. G. R. (1963) *Spectrochim. Acta* **19,** 2085–2092.
32. Pachler, K. G. R. (1964) *Spectrochim. Acta* **20,** 581–587.
33. Kessler, H., Griesinger, C. & Wagner, K. (1987) *J. Am. Chem. Soc.* **109,** 6927–6933.
34. Grant, D. M. & Cheney, B. V. (1967) *J. Am. Chem. Soc.* **89,** 5315–5318.
35. Wolfenden, W. R. & Grant, D. M. (1966) *J. Am. Chem. Soc.* **88,** 1496–1502.
36. Hansen, P. E., Batchelor, J. G. & Feeney, J. (1977) *J. Chem. Soc. Perkin Trans.* 50–54.
37. Momany, F. A., McGuire, R. F., Burgess, A. W. & Scheraga, H. A. (1975) *J. Phys. Chem.* **79,** 2361–2381.
38. Némethy, G., Pottle, M. S. & Scheraga, H. A. (1983) *J. Phys. Chem.* **87,** 1883–1887.
39. Dunfield, L. G., Burgess, A. W. & Scheraga, H. A. (1978) *J. Phys. Chem.* **82,** 2609–2616.
40. Weiner, S. J., Kollman, P. A., Case, D. A., Singh, U. C., Ghio, C., Alagona, G., Profeta, S. & Weiner, P. (1984) *J. Am. Chem. Soc.* **106,** 765–784.
41. Mohamadi, F., Richards, N. G. J., Guida, W. C., Liskamp, R., Lipton, M., Caufield, C., Chang, G., Hendrickson, T. & Still, W. C. (1990) *J. Computat. Chem.* **11,** 440–467.
42. Zimmerman, S. S., Pottle, M. S., Némethy, G. & Scheraga, H. A. (1977) *Macromolecules* **10,** 1–9.
43. *SYBYL Molecular Modeling Software, Theory Manual,* Version 6.0 (1992) TRIPOS Associates, Inc., St. Louis, MO.
44. Bystrov, V. F., Ivanov, V. T., Portnova, S. L., Balashova, T. A. & Ovchinnikov, Y. A. (1973) *Tetrahedron* **29,** 873–877.
45. Shenderovich, M. D., Nikiforovich, G. V., Saulitis, J. B. & Chipens, G. I. (1988) *Biophys. Chem.* **31,** 163–173.
46. Kessler, H. (1981) *Angew. Chem. Int. Ed. Engl.* **21,** 512–523.
47. Kövér, K. E., Jiao, D., Fang, S. & Hruby, V. J. (1993) *Magn. Reson. Chem.* **31,** 1072–1076.
48. Kabsch, W. (1976) *Acta Crystallogr. Sect. A* **A32,** 922–923.
49. Shuman, R. T., Gesellchen, P. D., Smithwick, E. L. & Frederickson, R. C. A. (1981) in *Peptides: Synthesis, Structure, Function,* Rich, D. H. & Gross, E., Eds., Pierce Chemical Co., Rockford, IL, pp. 617–620.